Journal of Materials Chemistry B

Accepted Manuscript

ROYAL SOCIETY OF CHEMISTRY

www.rsc.org/materialsB

Journal Name

RSCPublishing

ARTICLE

Killing cancer cells with nanotechnology: novel poly(I:C) loaded liposome-silica hybrid nanoparticles

Cite this: DOI: 10.1039/x0xx00000x

Received 00th January 2012,
Accepted 00th January 2012

DOI: 10.1039/x0xx00000x

www.rsc.org/

Valentina Colapicchioni,[a] Sara Palchetti,[b] Daniela Pozzi,[b]* Elettra Sara Marini,[c] Anna Riccioli,[c] Elio Ziparo,[c] Massimiliano Papi,[d] Heinz Amenitsch,[e] Giulio Caracciolo[b]*

Polyinosinic-polycytidylic acid (poly(I:C)) is a synthetic double-stranded RNA (dsRNA) analog able to induce apoptosis in different cancer cells by the activation of toll-like receptor 3 (TLR3) and cytosolic helicases retinoic acid inducible gene I (RIG-I) like receptor. In this work, we have synthesized and thoroughly characterized a core-shell liposome-silica hybrid (LSH) nanoparticle (NP) made of a silica core surrounded by a multicomponent cationic lipid bilayer. In view of *in vivo* applications, a variant with polyethyleneglycol (PEG) grafted to the lipid surface was also synthesized. Poly(I:C)-loaded LSH NPs were characterized and optimized in terms of their chemical-physical properties by using dynamic light scattering (DLS), micro-electrophoresis and transmission electron microscopy (TEM). The ability of this new technology to kill cancer cells was validated in PC3 prostate cancer and MCF7 breast cancer cells by MTT proliferation assay, flow cytometry and fluorescence confocal microscopy. We found that negatively charged poly(I:C)-loaded LSH NPs are more efficient than their liposome counterpart in eliminating cancer cells thus representing excellent candidates for both *in vitro* and *in vivo* drug delivery applications.

Introduction

One of the most important aims of oncology and cancer immunology is the activation of the immune system focused on inhibiting tumor growth and inducing cancer cell apoptosis.[1,2,3,4] Polyinosinic-polycytidylic acid (poly(I:C)), a synthetic double-stranded RNA (dsRNA) analog, has been studied for several years in view of its application in cancer immunotherapy. To date, it is well recognized that poly(I:C) is able to change cancer microenvironment and suppress tumor growth by innate and adaptive immune system activation.[5,6,7,8,9] Moreover, it has been demonstrated that poly(I:C) directly induces programmed cell death in different cancer cells.[10,11] These anticancer properties are explicated by the upregulation of tumor suppressor genes and the activation of cell apoptosis via toll-like receptor 3 (TLR3), retinoic acid inducible gene I (RIG-I) and melanoma differentiation-associated gene-5 (MDA5).[12,13,14] However, despite the adjuvant potential of poly(I:C) being widely known,[15] its clinical application may be a double-edged sword. This synthetic dsRNA suffers from being poorly immunogenic and toxic when administered systematically and in high dosages.[16] Nevertheless, the combination of poly(I:C) with an adequate delivery system seems to be a promising strategy to lower the drug dosage required and to improve its therapeutic index by enhancing its efficacy and/or increasing its tolerability in the body.[17] Encapsulation not only provides drugs protection from degradation but represents also a valid approach to increase cellular uptake. Among the plethora of current drug delivery systems, cationic lipids are particularly attractive due to their efficiency,[18] biocompatibility[19] and capability to potentiate the effect of immune adjuvants.[7,20,21] Cationic liposomes (CLs)-poly(I:C) complexes have been validated as an effective vaccine adjuvant approach for eliciting antiviral and antitumor immune responses.[22] In a recent study we have investigated the effect of lipid composition on the ability of (CLs)-poly(I:C) complexes to eliminate cancer cells.[17] However, liposome mechanical instability is a critical factor that does severely limit the efficiency of cargo delivery and release.[23] The possibility to synthesize a lipid shell and an enclosed solid core into a single particle architecture has gained significant attention because this hybrid design combines the merits of liposomes and inorganic materials while excluding some of their limits.[24] This synergistic combination ultimately provides mechanical

stability, controlled morphology, biodegradability, narrow size distribution and high drug loading capacity.[24] Silica nanoparticles (NPs) are highly attractive as a core because of their biocompatibility and possibility to electrostatically interact with CLs on one hand and on the other hand, for their capability to suppress large-scale bilayer fluctuations.[25] In order to further improve the anti-cancer activity of poly(I:C) by optimization of the nanodelivery system, in this work, we have designed and realized a core-shell liposome-silica hybrid (LSH) NP (Figure 1, panel A).

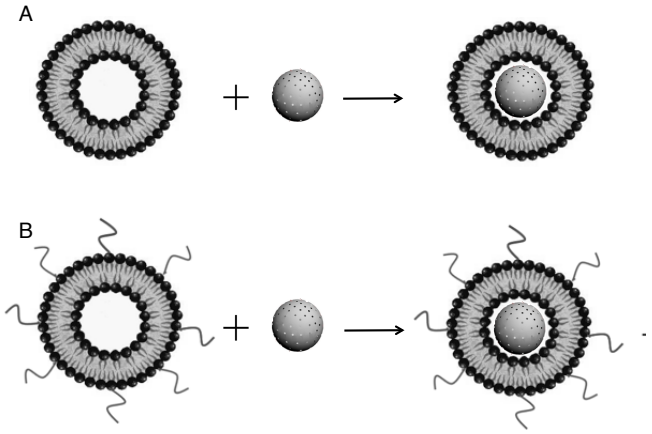

Figure 1. Schematic sketch describing the formation of liposome-silica hybrid (LSH) nanoparticles (NPs). (A) Multicomponent cationic liposomes were incubated with mesoporous silica nanoparticles. (B) Employment of pegylated liposomes results in the formation of pegylated LSH NPs.

To this end, mesoporous silica NPs were employed due to their peculiar ability to enhance lateral bilayer fluidity compared with that of either liposomes or supported lipid bilayers formed on non-porous cores.[25] Giving the superiority of multicomponent (MC) liposome in drug and gene delivery,[26,27] the lipid shell was made by a four-component lipid system constituted by cationic lipids 1,2-dioleoyl-3-trimethylammonium-propane (DOTAP) and (3β-[N-(N′,N′-dimethylaminoethane)-carbamoyl])-cholesterol (DC-Chol) and neutral helper lipids dioleoylphosphocholine (DOPC) and dioleoylphosphatidylethanolamine (DOPE). In view of *in vivo* application, a NP variant with polyethilenglycole (PEG) 2k grafted to the lipid shell was also designed (Figure 1, panel B).[28] To the best of our knowledge this is the first time that a liposome-silica hybrid system is employed as poly(I:C) delivery system and adjuvant. The anti-cancer activity of this core-shell hybrid nanoplatform was tested on the highly aggressive and androgen-independent prostate cancer cell line PC3, on which free poly(I:C) has only weak, if any, effect. Further validation was provided in MCF7 human breast adenocarcinoma cell line that is extensively used in cancer research. According to World Cancer Research Fund International (www.wcrf.org), prostate cancer and breast cancer are the fourth and the second most common cancers respectively, accounting for nearly 20 percent of all cancers. Notably, poly(I:C)-loaded LSH NPs were found to be highly efficient in eliminating cancer cells. At the lowest poly(I:C) dose, negative complexes were able to induce apoptosis in 40% of cancer cells. Remarkably, when cancer cells were treated with bare liposomes, a similar level of apoptosis required ten-fold the amount of poly(I:C).[17] Our results thus suggest that LSH NPs represent excellent candidates for both *in vitro* and *in vivo* drug delivery applications.

Results

Characterization of multicomponent liposomes

Size and zeta-potential experiments showed that both MC and MC-PEG2k CLs are positively charged small size vesicles (Table 1). Coating the MC surface with PEG2k resulted, as expected,[28] in a size increase (≈ 15 nm) and in a zeta-potential decrease (≈ 25 mV).

	D_H (nm)	zeta-potential (mV)
MC CLs	92.4±8.6	46.4±4.2
MC-PEG2k CLs	109.4±6.1	19.2 ±2.1

Table 1. Size and zeta-potential of unpegylated and pegylated multicomponent (MC) cationic liposomes (CLs).

To promote efficient interaction with silica NPs membrane unilamellarity of cationic vesicles is required. The technique of choice to test unilamellarity of liposomes in diluted solution is high-resolution synchrotron small angle X-ray scattering (SAXS). Figure 2 shows the synchrotron SAXS curves of both bare and pegylated MC CLs. As evident, MC lipid vesicles (Figure 2, bottom panel) exhibited only pure diffuse scattering, which is typical of uncorrelated bilayers. The scattered intensity was therefore fitted with one of the simplest lipid bilayer models[29] (further details about the fitting procedure are given in the Electronic Supplementary Information, ESI). The SAXS pattern of pegylated liposomes (Figure 2, top panel) revealed a slight deviation from the form factor at low q ($q < 1$ nm^{-1}). This observation is in line with previous studies showing that pegylated lipids can form phase-separated lamellae within lipid membranes.[30]

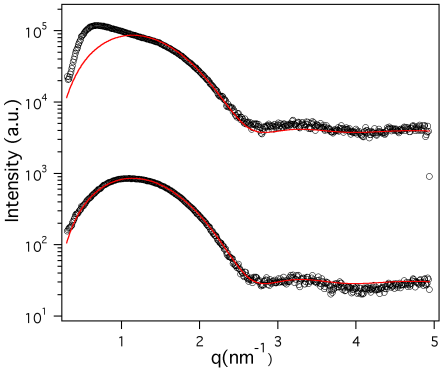

Figure 2. *Bottom panel*. Synchrotron SAXS pattern of unpegylated multicomponent cationic liposomes. *Top panel*. Synchrotron SAXS pattern of pegylated multicomponent cationic liposomes.

Mesoporous silica particles were found to be negatively charged (zeta-potential=-22.1±1.9 mV) and to have a hydrodynamic diameter D ≈ 440 nm. This size value is two-fold that reported by the manufacturer suggesting the presence of aggregates. The polydispersity index (PDI) (PDI=0.19) indicates that the suspension of mesoporous silica NPs is quite homogeneous in size. In Figure 3 (panel A), results of size characterization with transmission electron microscopy (TEM) and dynamic light scattering (DLS) techniques are reported.
TEM images show that mesoporous silica NPs are spherical in shape with an average hydrodynamic diameter D ≈ 200 nm and clearly visible nanopores. In addition, TEM results confirm the presence of aggregates as suggest by DLS.

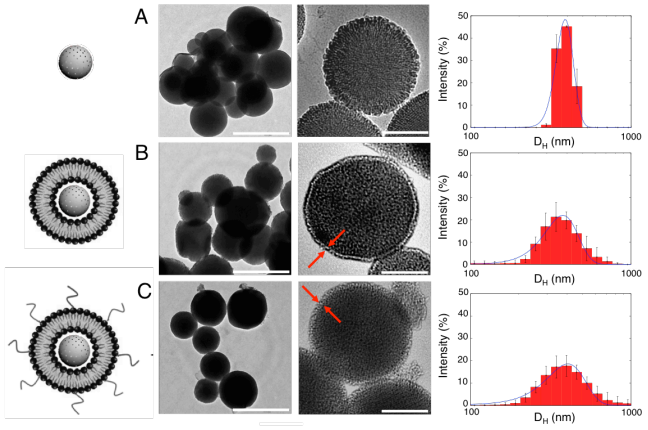

Figure 3. (A) Transmission electron microscopy (TEM) images of mesoporous silica NPs (scale bars 500 and 200 nm for left and right images respectively). Size distribution as determined by dynamic light scattering (DLS) (blue line is the best Gaussian fit to the data). (B) TEM images of liposome-silica hybrid (LSH) NPs (scale bars 500 and 200 nm for left and right images respectively). Size distribution of LSH NPs as determined by DLS (blue line is the best Gaussian fit to the data). A solid supported lipid bilayer (~ 4 nm thick) is indicated by red arrows (C) TEM images of pegylated LSH NPs (scale bars 500 and 200 nm for left and right images respectively). Size distribution of pegylated LSH NPs as determined by DLS (blue line is the best Gaussian fit to the data).

Formation of core-shell liposome-silica hybrid nanoparticles

Core-shell particles were realized by incubating MC CLs, both unpegylated and pegylated, with silica NPs (CLs:silica 1:5 w/w ratio) for 1 h. The electrostatic interaction between the two components resulted in the formation of a lipid shell around the silica core. Since this layer was found to be ≈ 4 nm thick (Figure 3B, right panel), we conclude, according to literature,[25] that it is a lipid bilayer. This was confirmed by zeta-potential experiments (zeta-potential=18.2±0.4 mV and 10.4±0.8 mV for unpegylated and pegylated NPs respectively). The adsorbed lipid shell made silica suspension less homogeneous in size as demonstrated by the both PDI (PDI ≈ 0.3) and DLS size distributions (Figure 3, right panels). DLS and TEM analyses supported each other in showing that pegylated and unpegylated LSH NPs are pretty similar in size (D≈300 nm) (Figure 3, panels B and C). The wider range of particle size exhibited by both unpegylated and pegylated LSH NPs may be due to local adsorption of lipid multilayers.

Loading core-shell liposome-silica hybrid nanoparticles with poly(I:C)

To rationally perform cell studies, the interaction between LSH NPs and poly(I:C) was investigated by size and zeta-potential experiments. Figure 4 shows the size and zeta-potential of both unpegylated and pegylated LSH NP/poly(I:C) complexes as a function of the poly(I:C)/lipid mass ratio, ρ. In all the experiments the amount of poly(I:C) was kept constant, while that of LSH NPs was varied.
Upon mixing, cationic LSH NPs and anionic poly(I:C) self-assemble in complexes whose size rapidly increases with increasing ρ. Simultaneously, complexes undergo the charge inversion effect, proven by the zeta-potential sign inversion occurring at ρ ≈ 0.025 and 0.075 for unpegylated and pegylated complexes respectively. When electro-neutrality is reached, van der Waals attraction dominates over electrostatic repulsion resulting in formation of large aggregates (D_H≈ 450 nm). Further increase of the poly(I:C) content (i.e. increasing ρ) induces charge inversion and re-entrant condensation of complexes up to saturation. Pegylation, creating a steric hindrance, weakens the interaction between RNA phosphates and cationic lipid headgroups thus boosting the drug necessary to reach the electro-neutrality. To generalize results, cancer cells were treated with negatively charged, neutral and positively charged complexes. Size and zeta-potential experiments allowed us to identify the proper ρ values to generate positive (ρ=0.05 for both the variants), neutral (ρ= 0.025 and 0.075 for unpegylated and pegylated LSH NPs respectively) and negative (ρ=0.25 for both the variants) complexes.

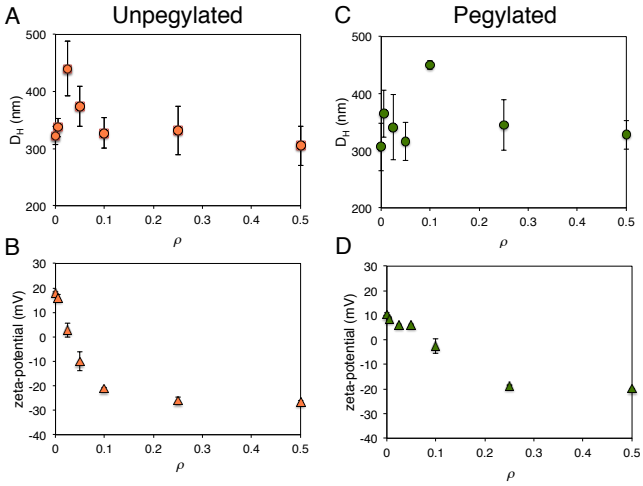

Figure 4. (A) Size of unpegylated poly(I:C)-loaded liposome-silica hybrid nanoparticles (LSH NPs) as a function of the poly(I:C)/cationic lipid mass ratio, ρ. (B) Zeta-potential of unpegylated poly(I:C)-loaded LSH NPs as a function of ρ. (C) Size of pegylated poly(I:C)-loaded LSH NPs as a function of ρ. (D) Zeta-potential of pegylated poly(I:C)-loaded LSH NPs as a function of ρ.

Anti-tumoral activity of poly(I:C)-loaded core-shell liposome-silica hybrid nanoparticles

It is well recognized that poly(I:C) is able to activate apoptosis in different cancer cells.[10,11] To validate our technology, two different cancer cell lines were selected. The highly aggressive and androgen-independent prostate cancer cell line PC3 and human breast adenocarcinoma MCF7 were chosen because on them free poly(I:C) has only weak, if any, apoptotic effect.[31] Also in MCF7 cells free poly(I:C) is ineffective. Both cancer cell lines were treated with poly(I:C)-loaded LSH NPs at three different poly(I:C) concentrations spanning one order of magnitude (0.2, 1 and 2 μg/ml). The highest poly(I:C) concentration (2 μg/ml) was chosen on the basis of an earlier study where we delivered poly(I:C) in cancer cells by using MC cationic liposomes.[17] Cancer cells were subjected to MTT assay and cell viability was evaluated at 24 hours after NPs' administration. Figure 5 shows that when PC3 and MCF7 cancer cells were treated with the lowest dose of poly(I:C) (0.2 μg/ml), both positively- and neutrally-charged poly(I:C)-loaded LSH NPs did not reduce cell viability, while negative complexes did (viability 75% and 70% for PC3 and MCF7 cancer cells respectively).

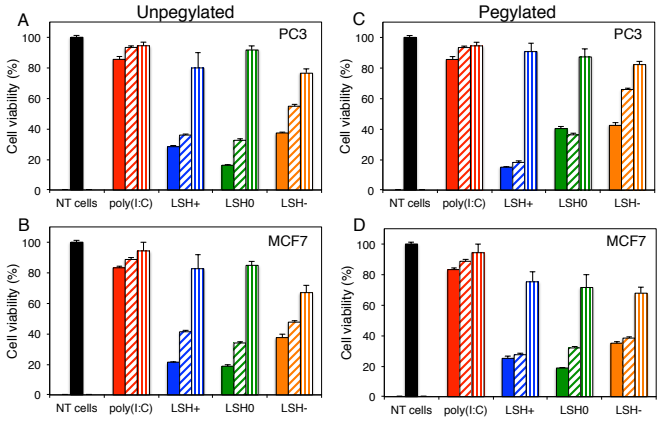

Figure 5. Cell viability of cancer cells after administration of positive, neutral and negative liposome-silica hybrid nanoparticles (LSH NPs) (LSH+, LSH0 and LSH- respectively) loaded with poly(I:C) at three different poly(I:C) concentrations spanning one order of magnitude: 2 (solid bars), 1 (diagonal dashed bars) and 0.2 (vertical dashed bars) μg/ml . Cell viability of unpegylated LSH NPs at 24 h after administration in PC3 and MCF7 cell lines (panels A and B). Cell viability of pegylated LSH NPs at 24 h after administration in PC3 and MCF7 cancer cell lines (panels C and D).

Since the corresponding bare LSH NPs (i.e. not loaded with poly(I:C)) did not appreciably affect cell viability (Figure S1 in the ESI), we suggest that negatively charged complexes have a distinct ability to induce apoptosis in cancer cells. It is note worthy to observe that bare MC liposomes need 10-fold more poly(I:C) to induce similar level of apoptosis in PC3 cancer cells.[17] At the highest poly(I:C) concentration (2 μg/ml), poly(I:C)-loaded LSH NPs exhibited high drug loading ability (Table S2 in the ESI) and significantly reduced cell viability of PC3 and MCF7 cancer cells with efficacy being in the order: positive>neutral>negative LSH NPs. Anyway, doses of positively- and neutrally-charged pristine LSH NPs had a significant cytotoxic effect on cells *per se* (cell viability ≈ 20-40%) (Figure S1 in the ESI). Bearing in mind that in all the experiments the amount of poly(I:C) was kept constant, while that of LSH NPs was varied, the observed trend in cell viability could not be related to the anticancer activity of poly(I:C), but to increased doses of potentially cytotoxic cationic NPs. Similar findings were obtained with pegylated LSH NPs (Figure 5 panels C and D).

Internalization of poly(I:C)-loaded core-shell liposome-silica hybrid nanoparticles in PC3 prostate cancer and MCF7 breast cancer cells

NP internalization is known to be a size-dependent process. Thus, we first investigated the effect of poly(I:C) loading on the size of LSH NPs. Representative TEM images (Figure 6 panels A and B) shows evidently the presence of a new shell onto the surface of both unpegylated and pegylated LSH NP/poly(I:C) complexes, recognizable as poly(I:C). In some cases, this layer of poly(I:C) acts as a glue forcing two NPs to come into contact. To further demonstrate the presence of both the lipid bilayer and the poly(I:C) layer over the core of the most efficient negative LSH NPs, we used an innovative set up which allows the combined acquisition of scanning electron microscopy (SEM) micrographs and X-ray Fluorescence (XRF) spectra. While SEM micrographs allow imaging the sample by scanning it with a focused beam of electrons, XRF allows obtaining a quantitative analysis of chemical elements within the sample. Figure 6 panels C and D show representative SEM micrographs of silica NPs (left panel) and poly(I:C)-loaded LSH NPs both unPEGylated (middle panel) and PEGylated (right panel). As expected, silica NPs contain almost exclusively silicon (red), with minor carbon contaminations (green). On the other side, XRF microanalysis showed the abundant presence of carbon on the surface of poly(I:C)-loaded LSH NPs in the order: unPEGylated < PEGylated. In the combined micrographs, yellow arises from colocalization of silicon and carbon with color tonality depending on the relative abundance of the chemical elements. As evident, XRF unambiguously showed the presence of carbon over poly(I:C)-loaded LSH NPs. This is due to carbon-rich macromolecules such as, lipids and poly(I:C). By means of dedicated software we quantified the relative abundance of both silicon and carbon. The higher abundance of carbon on the surface of PEGylated LSH NPs with respect to their unPEGylated counterpart (Figure 6, panel D) was most likely due to the presence of PEG whose basic structure is carbon-enriched.Subsequently, to discriminate between specific anti-cancer activity (i.e. due to poly(I:C)) and not specific cytotoxic effect (i.e. due to toxicity of cationic charge), we investigated the cellular uptake of poly(I:C)-loaded LSH NPs by combined flow cytometry and confocal microscopy experiments. To this end, poly(I:C)-loaded LSH NPs were doubly labeled by using NBD-labeled liposomes (green) and rhodamine-labeled poly(I:C) (red). Internalization was evaluated by flow cytometry experiments after 3 h ofincubation. Cellular uptake results are shown as the percentage of fluorescent positive cells in Figure 6.

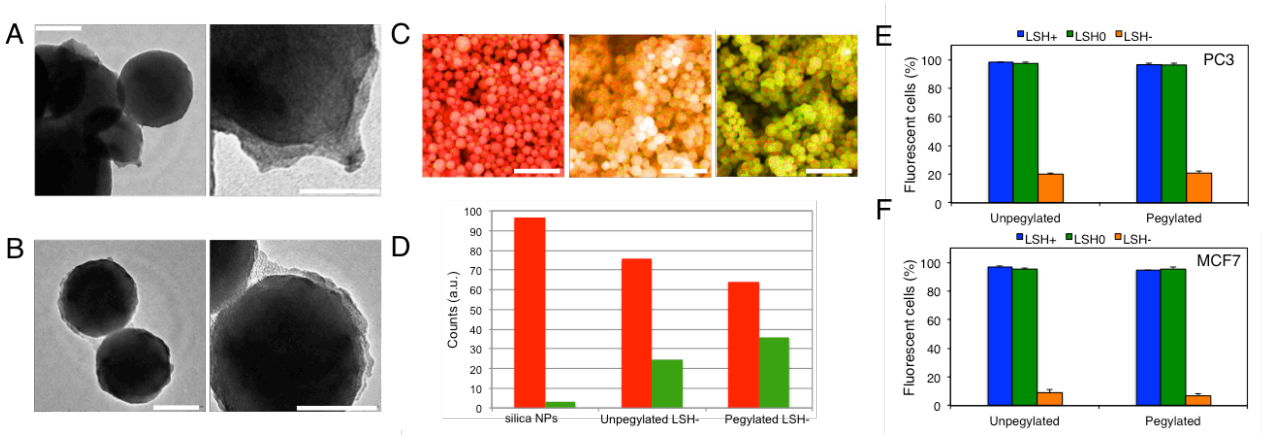

Figure 6. Transmission electron microscopy images of unpegylated (panel A) and pegylated (panel B) negatively charged LSH NP/poly(I:C) complexes. (Panel C) SEM micrographs of silica NPs (left panel), unPEGylated poly(I:C)-loaded LSH NPs (middle panel) and PEGylated poly(I:C)-loaded LSH NPs (right panel). (Panel D) Relative abundance of silicon (red) and carbon (green) within samples. Percentage of fluorescent cells in PC3 (panel E) and MC7 cell lines (panel F) of unpegylated and pegylated LSH NPs.

When cancer cells were treated with both positive and neutral LSH NPs, being indifferently unpegylated and pegylated, the percentage of fluorescent cells was much higher (>95%) than those of unpegylated and pegylated negatively charged complexes (20% and 10% respectively). To confirm that fluorescently labeled complexes were actually in the cytoplasm of PC3 and MCF7 cancer cells, confocal images were acquired (Figure 7). Confocal images of Figure 7 show that large clusters of positive and neutral LSH NPs are prevalently accumulated at the plasma membrane (white arrows) with no clear evidence of cellular internalization.

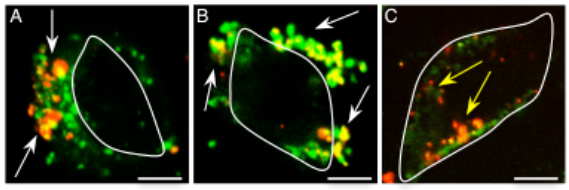

Figure 7. Representative confocal images of PC3 prostate cancer cells treated with doubled fluorescently-labeled unpegylated complexes (rhodamine-labeled poly(I:C) in red and NBD liposomes in green) (scale bars 2 µm). Panel A, positively charged complexes. Panel B, neutrally charged complexes. Panel C, negatively charged complexes. White arrows indicate complexes accumulated at the plasma membrane of cancer cells, while yellow arrows point toward complexes internalized within cancer cells.

Clusters were likely due to the large number of nanoparticles Indeed, in all the experiments the amount of poly(I:C) was kept constant because a correct comparison between the efficiencies of designed formulations requires that the same amount of drug be delivered. Negatively-, neutrally- and positively-charged LSH NPs were therefore prepared by adjusting the total positive charge of cationic lipids, i.e. by increasing the number of NPs. On the other hand, both unpegylated and pegylated negative LSH NPs were mainly internalized within cancer cells (yellow arrows). Moreover, the presence of abundant yellow/orange structures arising from colocalization of red and green fluorescence demonstrates that poly(I:C)-loaded LSH NPs complexes are stable within cancer cells.

Discussion

Poly(I:C), a synthetic analog of dsRNA, has been studied in tumor immunotherapy for several decades. The accumulated evidence suggests that poly(I:C) not only enhances innate and adaptive immune responses and alters the tumor microenvironment, but also directly triggers apoptosis in cancer cells through activation of TLR3 and RIG-I-like receptors signaling pathways.[5,32,33] However, stability and toxicity issues so far prevented the clinical application of this synthetic dsRNA as it undergoes rapid enzymatic degradation and bears the potential to trigger undue immune stimulation as well as autoimmune disorders.[16] Hence, poly(I:C) calls for efficient delivery systems able to lower its necessary dosage and to improve its therapeutic index by enhancing its efficacy and/or increasing its tolerability in the body. In this work, we developed a LSH nanoplatform to deliver poly(I:C) in cancer cells. It is a synergistic system resulting from the fusion of highly efficient multicomponent CLs on negatively charged mesoporous silica NPs to form a core-shell structure. Despite different models of liposome-based formulations such as polymer-coated liposomes,[34] hydrogel/liposome composites[35] and nanoparticle-stabilized liposomes[36] have been developed, mesoporous silica is particularly attractive as support because of its ability to decrease large-scale bilayer fluctuations that are co-responsible for rapid vesicle clearance *in vivo*.[25] Our DLS and TEM analysis (Figure 3) showed that silica NPs had a precisely defined nanoporosity and shape. Their negative surface charge let these particles favorably interact with CLs. Compared to other delivery vectors, the LSH NP is simple to synthesize and takes advantage of the low toxicity, versatility and immunogenicity of liposomes. Compared to

bare liposomes, however, the LSH NPs are more stable and homogeneous in size due to the silica core.[37] As a lipid shell, MC CLs were chosen due to their superiority to deliver drugs and genes both *in vitro* and *in vivo*.[26, 27] Furthermore, MC CLs have shown a tendency to adsorb apolipoproteins onto their surface when in contact with a biological milieu.[28] This class of proteins plays a very important biological role, since they are able to bind to target cell receptors such as the low density lipoprotein (LDL) receptor, scavenger receptor class B type 1 receptor and the transferrin receptor thus resulting in efficient transport across biological barriers such as the blood–brain barrier.[38,39,40] Combined DLS, zeta-potential and TEM results demonstrated that the experimental procedure allowed obtaining a population of LSH NPs quite homogeneous both in size (≈ 300 nm) and charge (≈18.2 mV). Notably, the protocol did not result in free liposomes coexisting with LSH NPs (data not reported). The absence of free liposomes is mandatory to evaluate the core-shell NP performance without any contribution/interference arising from free cationic vesicles. Nonetheless, the LSH particles we synthesized are particularly attractive because of their good stability in time within 48 hours from preparation (data not reported for space consideration). In view of *in vivo* applications, we also developed a "stealth" variant of LSH NPs by using MC CLs grafted with PEG2k. Pegylation had a minor effect on the size and charge of MC CLs (Table 1). At present PEGylation represents the most efficient strategy to increase NPs pharmacokinetics.[41] Linear chains of this polymer, grafted on liposome surface, make these vectors able to evade immune system interception by reducing non-specific protein adsorption and opsonization that is responsible of the activation of the mononuclear phagocytes. On the other side, some authors are questioning the use of PEGylation in drug delivery since it can cause reduced uptake by target cells, and a dose-dependent elicitation of an immune response that facilitates clearance *in vivo*.[42] The same authors suggest that novel strategies based on the presence of cholesterol nanodomains within the lipid bilayer could help towards improving performances of liposomes.[43] After identifying a lipid blend assuring reduced non-specific protein adsorption and opsonization, this could be used to synthesize LSH NPs with optimized pharmacokinetics profiles. After characterizing LSH NPs in full (Figure 3), we applied DLS and micro-electrophoresis to investigate the interaction between positively charged LSH NPs and negatively charged poly(I:C). Since the interaction between cationic lipid headgroups of LSH NPs and the phosphates of poly(I:C) is dominated by electrostatic interactions leading to complexes of varying charge and size, micro-electrophoresis and DLS are the best techniques to unravel the phenomenology of complexation. Size and zeta-potential of LSH NP/poly(I:C) complexes were investigated as a function of the poly(I:C)/lipid weight ratio, ρ and allowed us to identify ρ ratios to generate negatively-, neutrally- and positively-charged complexes. As shown in the Figure 4, charge inversion takes place at very low ρ values, namely 0.025 and 0.05 for unpegylated and pegylated NPs respectively. This means that, at fix cationic lipid, pegylated LSH NPs require 2-fold amount of poly(I:C) to reverse charge. This behavior can be justified considering that the linear PEG chains grafted on the lipid shell are able to create steric hindrance,[44,45] resulting in a significant inhibition of poly(I:C) adsorption. To validate this new technology, poly(I:C)-loaded LSH NPs were given to prostate PC3 and breast MCF7 cancer cell lines. According to worldwide statistics (www.wcrf.org), prostate cancer and breast cancer are the fourth and the second most common cancers respectively with nearly three millions new cases each year. More in detail, PC3 cell line is one of the most used cell lines in prostate cancer research due to their high metastatic potential. Likewise, the popularity of MCF7 is largely due to its peculiar hormone sensitivity through expression of estrogen receptor (ER) that makes it an ideal model to study hormone response. Preliminary MTT experiments were performed treating both PC3 and MCF7 cancer cells with bare LSH NPs (i.e. not loaded with poly(I:C)). Figure S1 in the ESI showed that doses of NPs needed to produce positively- and neutrally-charged complexes have a significant cytotoxic effect on the cells. High cytotoxicity was likely due to the high dose of cationic lipid concentration. On the other hand, when PC3 and MCF7 cancer cells were treated with the low dose of LSH NPs needed to generate negatively charged complexes, minor, if any, cytotoxicity was observed. Figure 5 shows that negative LSH NP/poly(I:C) complexes were much more efficient in inducing apoptosis with respect to the free drug. Notably, negative complexes with the lowest poly(I:C) concentration (0.2 μg/ml) were able to induce appreciable levels of apoptosis. At the same poly(I:C) concentration, both positively- and neutrally-charged poly(I:C)-loaded LSH NPs did not appreciably kill cancer cells. Since the corresponding pristine LSH NPs (i.e. not loaded with poly(I:C)) did not appreciably affect cell viability (Figure S1 in the ESI), we deduced that negatively charged LSH NP/poly(I:C) complexes have a peculiar ability to induce apoptosis in cancer cells. Moreover, it is note worthy to observe that bare MC liposomes needed about 10-fold more poly(I:C) to induce similar levels of apoptosis.[17] At the highest poly(I:C) concentration (2 μg/ml), poly(I:C)-loaded LSH NPs exhibited high efficiency in eliminating both PC3 and MCF7 cancer cells. Nonetheless, positively- and neutrally-charged bare LSH NPs remarkably affected cell viability per se (Figure S1 in the ESI) showing that the observed reduction in cell viability was due to cytotoxic cationic lipids more than to poly(I:C). To distinguish between specific anti-cancer activity of poly(I:C) and not specific cytotoxicity of cationic charge, we explored the cellular uptake of poly(I:C)-loaded LSH NPs by combined flow cytometry and fluorescence confocal microscopy. To this end, poly(I:C)-loaded LSH NPs were doubly labeled by using NBD-labeled liposomes (green) and rhodamine-labeled poly(I:C) (red).

When PC3 prostate and MCF7 breast cancer cells were treated with both positive and neutral LSH NPs, being indifferently unpegylated and pegylated, the percentage of fluorescent cells was much higher (>95%) than those of negative complexes (Figure 6, panels C and D). Confocal microscopy (Figure 7) clarified that positive and neutral complexes were prevalently accumulated at the plasma membrane (white arrows) with no clear evidence of cellular internalization, while negative ones were mainly internalized within cancer cells (yellow arrows). This conclusive set of experiments allowed to identify the higher cellular uptake of negative LSH NP/poly(I:C) complexes as the rational basis of their peculiar ability to eliminate PC3 prostate and MCF7 breast cancer cells. In addition confocal microscopy allowed us to understand that positive and neutral LSH NP/poly(I:C) reduced cell viability of PC3 and MCF7 cancer cells mainly due to unspecific cytotoxicity of cationic lipid charge. Lastly, confocal images reported in Figure 7 showed that red and green fluorescence signals were colocalized. This means that synthesized core-shell NPs have a minor, if any, ability to fuse with the membranes of endosomes and release their poly(I:C) cargo. According to recent findings,[17] release of poly(I:C) in the cytosol seems not to be a limiting factor to induce apoptosis in cancer cells. Indeed, we have recently demonstrated that the prominence of receptors localized in the endosomes (e.g. TLR-3) with respect to cytosolic receptors in activating apoptotic cascade signaling pathways.[46]

Experimental

Multicomponent cationic liposomes preparation

1,2-dioleoyl-3-trimethylammonium-propane (DOTAP) and (3β-[N-(N′,N′-dimethylaminoethane)-carbamoyl])-cholesterol (DC-Chol), dioleoylphosphocholine (DOPC), dioleoylphosphatidylethanolamine (DOPE), DOPE-polyethyleneglycol (PEG) 2k were purchased from Avanti Polar Lipids (Alabaster, AL) and used without further purification. Liposomes were prepared in accordance with standard procedures[47, 48] by dissolving appropriate amounts of lipids at ϕ = neutral lipid/total lipid (mol/mol) = 0.5. MC liposomes were synthesized according with these molar ratios DOTAP:DOPC:DC-Chol:DOPE (1:1:1:1) and DOTAP:DOPC:DC-Chol:DOPE:DOPE-PEG2k (1:1:1:0.7:0.3). For laser scanning confocal microscopy (LSCM) and flow cytometry experiments, NBD-DOPE was mixed with unlabeled DOPE to obtain labeled MC liposomes. In all the samples the concentration of fluorescently labeled NBD-DOPE was fixed at 7×10^{-3} mg/mL (fluorescent lipid/total lipid molar ratio ≈ 5/1000). Lipid films were hydrated (final lipid concentration 1 mg/mL) with phosphate buffered saline (PBS).

Synthesis of liposome-silica hybrid nanoparticles

Mesoporous silica NPs were purchased from Sigma Aldrich and resuspended in ultrapure water (final concentration 1mg/mL). Silica suspension was incubated with CLs (1mg/mL in PBS) for 1 h at room temperature according with this weight ratio MC liposome (both pegylated and unpegylated):silica 1:5 (w/w).

Size and zeta-potential experiments

All size and zeta-potential measurements were made at 25°C on a Zetasizer Nano ZS90 (Malvern, U.K.) spectrometer equipped with a 5 mW HeNe laser (wavelength λ = 632.8 nm) and a digital logarithmic correlator. The normalized intensity autocorrelation functions were analyzed by using the CONTIN method,[49] which analyzes the autocorrelation function through an inverse Laplace transform in order to obtain the distribution of the diffusion coefficient D of the particles. This coefficient is converted into an effective hydrodynamic radius R_H by using the Stokes-Einstein equation $R_H = K_BT/(6\pi\eta D)$, where K_BT is the thermal energy and η is the solvent viscosity. The electrophoretic mobility measurements were performed by means of the laser Doppler electrophoresis technique, by the same apparatus used for size measurements. The mobility u was converted into the zeta-potential by using the Smoluchowski relation zeta-potential = $u\eta/\varepsilon$, where η and ε are respectively the viscosity and the permittivity of the solvent phase. Results are given as mean ± standard deviation of three replicates.

Synchrotron Small Angle X-ray Scattering (SAXS)

SAXS experiments were performed at the Austrian SAXS beam line of the synchrotron light source ELETTRA (Trieste, Italy).[50] SAXS patterns were recorded with gas detectors spanning the q-ranges from $q_{min} = 0.005$ nm^{-1} to $q_{max} = 5$ nm^{-1} with a resolution of 5×10^{-3} nm^{-1} (fwhm). The angular calibration of the detectors was performed with silver behenate powder (d-spacing of 58.38 Å). The data have been properly normalized.[51, 52] Usually exposure times were 10 s. No evidence of radiation damage was observed in the SAXS patterns. The sample was held in a 1 mm glass capillary (Hilgenberg, Malsfeld, Germany) and the measurements were executed at room temperature.

Transmission electron microscopy (TEM)

Samples for TEM were prepared as elsewhere described.[53] Briefly, a small drop (10 μL) of the suspension was dispersed on carbon-coated copper grids. All the samples were allowed to adsorb on the carbon film for 1 min and after was stained with a 2% uranyl acetate solution for 30 s in the dark at room temperature. Excess of staining was adsorbed with a filter paper, and grids were allowed to air dry for 1 h before observation.

Scanning electron microscopy (SEM) and X-ray Fluorescence (XRF)

A small drop (10 μL) of the suspension was dispersed on a double-sided adhesive conductive carbon disc and dried at room temperature. For nanoparticle investigation scanning electron microscope Zeiss Supra 25 (Germany) equipped with energy dispersive spectroscope (EDS) was used. Accelerating voltage in the range of 3 to 20 kV was set, depending on the applied magnification as well the phase contrast of the areas of interest. Further details can be found elsewhere.[54]

Liposome-silica hybrid nanoparticles/poly(I:C) complexes

Poly(I:C) purchased from Invivogen (San Diego, CA), was used. By mixing adequate amounts of the poly(I:C) solutions to suitable volumes of LSH dispersions, LSH NP/poly(I:C) complexes were obtained at several CLs/poly(I:C) weight ratios (w/w). For laser scanning confocal microscopy rhodamine-labeled poly(I:C) (Invivogen) was used.

Cell Line experiments

Human prostate cancer (PC3) cell line, derived from human bone prostate cancer metastasis, was purchased from ATCC (Manassas, VA, USA). PC3 cells were maintained in RPMI 1640 medium supplemented with 2 mM L-glutamine, 100 IU/mL penicillinstreptomycin, 1 mM sodium pyruvate, 10 mMhepes, 1.5 mg/L sodium bicarbonate, and 10% fetal bovine serum (FBS) (Sigma-Aldrich, St. Louis, MO, USA). Michigan Cancer Foundation 7 (MCF7) cell line, derived from human pleural effusion metastasis, was purchased from ATCC (Manassas, VA, USA). MCF7 cells were maintained in Eagle's Minimum Essential Medium (EMEM) (Sigma Aldrich, St. Louis, MO, USA) supplemented with 0.01 mg/ml human recombinant insulin and 10% fetal bovine serum (FBS).

Analysis of Cell Viability

In cell viability experiments, the amount of poly(I:C) was kept constant because a correct comparison between the efficiencies of designed formulations requires that the same amount of drug be delivered. Negatively-, neutrally- and positively-charged LSH NPs were therefore prepared by adjusting the total positive charge of cationic lipids, i.e. by merely increasing the amount of NPs. In the absence of poly(I:C), cells were treated with the same amount of LSH NPs we used to prepare negative, neutral and positive NPs respectively. This was the most logical choice to investigate the potential toxicity arising from undecorated LSH NPs. Cell viability of PC3 and MCF7 cells was assessed by 3-(4,5-dymethyl thiazol 2-y1)-2,5-diphenyl tetrazolium bromide (MTT, mitochondrial respiration analysis; Sigma-Aldrich), according to Mosmann protocol. Briefly, PC3 and MCF7 cells were seeded on 96-wells plate and treated with LSH-poy(I:C) complexes for 24 hours. MTT was added to each well at the final concentration of 0.5 mg/mL and after 4 hours of incubation at 37°C, the formazan salt was dissolved with 100 μL is opropylic alcohol. The absorbance of each well was measured with Glomax Discover System (Promega, Madison, WI, USA), a high-performance multimode detection instrument. The viability was calculated for each treatment as "OD of treated cells/OD of control cells" ×100.

Flow Cytometry

200.000 cells/mL/well were plated in 12-well dishes. After 24 h, PC3 and MCF7 cells were incubated for 3h with double labeled platforms: realized using NBD liposomes and rhodamine-labeled poly(I:C) (Invivogen,San Diego, CA). After the treatment the cells were detached with trypsin/ethylenediaminetetraacetic acid (EDTA), washed two times with cold PBS, and run on a cyan cytometer (Beckman Coulter, Fullerton, CA, USA). Data were analyzed using FCS3 express software (De NovoSoftware, Los Angeles, CA, USA).

Laser Scanning Confocal Microscopy (LSCM)

PC3 and MCF7 cells were seeded onto 12-mm round glass coverlips and incubated with fluorescently labeled LSH NPs complexes for 3 h. Then cells were fixed in paraformaldehyde 4% in phosphate-buffered saline (PBS) (Sigma-Aldrich, St. Louis, MO, USA) for 20 min. LSCM experiments were performed with a Leica TCS SP2 (Leica Microsystems Heidelberg GmbH, Germany).

Conclusions

We have designed, synthesized and thoroughly characterized a versatile core-shell liposome-silica hybrid nanoparticle made of a silica core surrounded by a multicomponent cationic lipid bilayer. This "organic-inorganic" hybrid material combines the merits of silica nanoparticles (mechanical stability, controlled morphology and narrow size distribution) with the intrinsic biocompatibility and superior gene delivery performances of multicomponent cationic liposomes. To validate this technology, core-shell liposome-silica hybrid nanoparticles were loaded with poly(I:C), a synthetic dsRNA analog that is able to modify cancer microenvironment and suppress tumor growth by innate and adaptive immune system activation. Both unpegylated and pegylated poly(I:C)-loaded LSH NPs have a distinct skill in eliminating human PC3 prostate cancer and MCF7 breast cancer cells. Remarkably, negatively charged LSH NPs with an extremely low poly(I:C) concentration (0.2 mg/ml/well) were able to efficiently kill cancer cells. It is notable that bare liposomes required 10-fold more poly(I:C) to induce similar level of apoptosis. Thus, we conclude that LSH NPs represent very promising candidates for both *in vitro* and *in vivo* drug delivery applications.

Acknowledgements

GC and DP acknowledge support by the Italian Minister for University and Research ("Futuro in Ricerca 2008", Grant no. RBFR08TLPO). VC, DP and GC acknowledge support by the Istituto Italiano di Tecnologia, Center for Life Nano Science@Sapienza.

Notes and references

[a]*Center for Life Nano Science@Sapienza, Istituto Italiano di Tecnologia*
Viale Regina Elena 291, 00161 Roma, Italy.
[b]*Department of Molecular Medicine, 'Sapienza' University of Rome, Viale Regina Elena 291, 00161 Rome, Italy*
[c]*Istituto Pasteur-Fondazione Cenci Bolognetti, Department of Anatomy, Histology, Forensic Medicine and Orthopaedics, Section of Histology and Medical Embryology, 'Sapienza' University of Rome, Via A. Scarpa 14, 00161 Rome, Italy*
[d]*Istituto di Fisica, Università Cattolica del Sacro Cuore, Largo F. Vito 1, 00168 Rome, Italy*
[e]*Institute of Inorganic Chemistry, Graz University of Technology, Stremayerg. 6/IV, 8010 Graz, Austria*

*E-mail: giulio.caracciolo@uniroma1.it; daniela.pozzi@uniroma1.it

Electronic Supplementary Information (ESI) available: Fitting procedure of synchrotron small angle X-ray scattering data with results shown in Table S1. Figure S1 Counterpart of Figure 5 for bare NPs (i.e. not loaded with poly(I:C)). In Table S2 the poly(I:C) encapsulation efficiency is reported. See DOI: 10.1039/x0xx00000x

1. J. N. Blattman and P. D. Greenberg, *Science*, 2004, **305**, 200-205.
2. C. H. June, *Journal of Clinical Investigation*, 2007, **117**, 1466-1476.
3. L. M. Weiner, R. Surana and S. Wang, *Nature Reviews Immunology*, 2010, **10**, 317-327.
4. Y. S. Cheng and F. Xu, *Cancer Biology and Therapy*, 2010, **10**, 1219-1223.
5. A. I. Chin, A. K. Miyahira, A. Covarrubias, J. Teague, B. Guo, P. W. Dempsey and G. Cheng, *Cancer Research*, 2010, **70**, 2595-2603.
6. J. Tissari, J. Sirén, S. Meri, I. Julkunen and S. Matikainen, *Journal of Immunology*, 2005, **174**, 4289-4294.
7. M. Yoneyama, M. Kikuchi, K. Matsumoto, T. Imaizumi, M. Miyagishi, K. Taira, E. Foy, Y. M. Loo, M. Gale Jr, S. Akira, S. Yonehara, A. Kato and T. Fujita, *Journal of Immunology*, 2005, **175**, 2851-2858.
8. M. Matsumoto and T. Seya, *Advanced Drug Delivery Reviews*, 2008, **60**, 805-812.
9. T. Kawai and S. Akira, *Annals of the New York Academy of Sciences*, 2008, **1143**, 1-20.
10. B. Salaun, I. Coste, M. C. Rissoan, S. J. Lebecque and T. Renno, *Journal of Immunology*, 2006, **176**, 4894-4901.
11. B. Salaun, S. Lebecque, S. Matikainen, D. Rimoldi and P. Romero, *Clinical Cancer Research*, 2007, **13**, 4565-4574.
12. R. Besch, H. Poeck, T. Hohenauer, D. Senft, xE, G. cker, C. Berking, V. Hornung, S. Endres, T. Ruzicka, S. Rothenfusser and G. Hartmann, *The Journal of Clinical Investigation*, 2009, **119**, 2399-2411.
13. K. Hirabayashi, J. Yano, T. Inoue, T. Yamaguchi, K. Tanigawara, G. E. Smyth, K. Ishiyama, T. Ohgi, K. Kimura and T. Irimura, *Cancer Research*, 1999, **59**, 4325-4333.
14. T. Fujimura, S. Nakagawa, T. Ohtani, Y. Ito and S. Aiba, *European Journal of Immunology*, 2006, **36**, 3371-3380.
15. K. Tewari, B. J. Flynn, S. B. Boscardin, K. Kastenmueller, A. M. Salazar, C. A. Anderson, V. Soundarapandian, A. Ahumada, T. Keler, S. L. Hoffman, M. C. Nussenzweig, R. M. Steinman and R. A. Seder, *Vaccine*, 2010, **28**, 7256-7266.
16. A. M. Hafner, B. Corthésy and H. P. Merkle, *Advanced Drug Delivery Reviews*, 2013, **65**, 1386-1399.
17. S. Palchetti, D. Pozzi, A. Riccioli, E. Ziparo, V. Colapicchioni, H. Amenitsch and G. Caracciolo, *RSC Advances*, 2013, **3**, 24597-24604.
18. E. Junquera and E. Aicart, *Current topics in medicinal chemistry*, 2014.
19. W. T. Al-Jamal and K. Kostarelos, *Accounts of Chemical Research*, 2011, **44**, 1094-1104.
20. S. Garg, E. Valente, E. Greco, M. Santucci, M. De Spirito, M. Papi, M. Bocchino, C. Saltini and M. Fraziano, *Clinical immunology*, 2006, **121**, 23-28.
21. E. Greco, M. B. Santucci, M. Sali, F. R. De Angelis, M. Papi, M. De Spirito, G. Delogu, V. Colizzi and M. Fraziano, *Immunology*, 2010, **129**, 125-132.
22. P. Nordly, F. Rose, D. Christensen, H. M. Nielsen, P. Andersen, E. M. Agger and C. Foged, *Journal of Controlled Release*, 2011, **150**, 307-317.
23. M. Liu, L. Gan, L. Chen, Z. Xu, D. Zhu, Z. Hao and L. Chen, *Langmuir*, 2012, **28**, 10725-10732.
24. W. Gao, C. M. J. Hu, R. H. Fang and L. Zhang, *Journal of Materials Chemistry B*, 2013, **1**, 6569-6585.
25. C. E. Ashley, E. C. Carnes, G. K. Phillips, D. Padilla, P. N. Durfee, P. A. Brown, T. N. Hanna, J. Liu, B. Phillips, M. B. Carter, N. J. Carroll, X. Jiang, D. R. Dunphy, C. L. Willman, D. N. Petsev, D. G. Evans, A. N. Parikh, B. Chackerian, W. Wharton, D. S. Peabody and C. J. Brinker, *Nat Mater*, 2011, **10**, 389-397.
26. D. Pozzi, C. Marchini, F. Cardarelli, A. Rossetta, V. Colapicchioni, A. Amici, M. Montani, S. Motta, P. Brocca, L. Cantù and G. Caracciolo, *Molecular Pharmaceutics*, 2013, **10**, 4654-4665.
27. G. Caracciolo, D. Pozzi and R. Caminiti, *Applied Physics Letters*, 2006, **89**.
28. D. Pozzi, V. Colapicchioni, G. Caracciolo, S. Piovesana, A. L. Capriotti, S. Palchetti, S. De Grossi, A. Riccioli, H. Amenitsch and A. Laganà, *Nanoscale*, 2014, **6**, 2782-2792.
29. G. Pabst, M. Rappolt, H. Amenitsch and P. Laggner, *Physical Review E*, 2000, **62**, 4000.
30. K. Hashizaki, H. Taguchi, C. Itoh, H. Sakai, M. Abe, Y. Saito and N. Ogawa, *Chemical and pharmaceutical bulletin*, 2003, **51**, 815-820.
31. D. L. Holliday and V. Speirs, *Breast Cancer Res*, 2011, **13**, 215.
32. S. Koyama, K. J. Ishii, H. Kumar, T. Tanimoto, C. Coban, S. Uematsu, T. Kawai and S. Akira, *Journal of Immunology*, 2007, **179**, 4711-4720.
33. H. Kumar, S. Koyama, K. J. Ishii, T. Kawai and S. Akira, *The Journal of Immunology*, 2008, **180**, 683-687.
34. S. Rameez and A. F. Palmer, *Langmuir*, 2011, **27**, 8829-8840.
35. N. MacKinnon, G. Guérin, B. Liu, C. C. Gradinaru and P. M. Macdonald, *Langmuir*, 2009, **25**, 9413-9423.
36. N. Zhang, Q. Ping, G. Huang, W. Xu, Y. Cheng and X. Han, *International Journal of Pharmaceutics*, 2006, **327**, 153-159.
37. J. Liu, A. Stace-Naughton, X. Jiang and C. J. Brinker, *Journal of the American Chemical Society*, 2009, **131**, 1354-1355.
38. M. P. Monopoli, F. B. Bombelli and K. A. Dawson, *Nature Nanotechnology*, 2011, **6**, 11-12.
39. E. Hellstrand, I. Lynch, A. Andersson, T. Drakenberg, B. Dahlbäck, K. A. Dawson, S. Linse and T. Cedervall, *FEBS Journal*, 2009, **276**, 3372-3381.
40. V. Zannis, A. Chroni and M. Krieger, *J Mol Med*, 2006, **84**, 276-294.
41. A. Vonarbourg, C. Passirani, P. Saulnier and J.-P. Benoit, *Biomaterials*, 2006, **27**, 4356-4373.
42. J. J. Verhoef and T. J. Anchordoquy, *Drug Delivery and Translational Research*, 2013, **3**, 499-503.
43. J. L. Betker, M. Kullberg, J. Gomez and T. J. Anchordoquy, *Therapeutic delivery*, 2013, **4**, 453-462.
44. J. Satulovsky, M. A. Carignano and I. Szleifer, *Proceedings of the National Academy of Sciences*, 2000, **97**, 9037-9041.

45. I. Szleifer, *Biophysical Journal*, 1997, **72**, 595-612.
46. S. Palchetti, D. Starace, P. De Cesaris, A. Filippini, E. Ziparo and A. Riccioli, *Journal of Biological Chemistry*, 2015, jbc. M114. 601625.
47. D. Pozzi, C. Marchini, F. Cardarelli, H. Amenitsch, C. Garulli, A. Bifone and G. Caracciolo, *Biochimica et Biophysica Acta (BBA) - Biomembranes*, 2012, **1818**, 2335-2343.
48. G. Caracciolo, F. Cardarelli, D. Pozzi, F. Salomone, G. Maccari, G. Bardi, A. L. Capriotti, C. Cavaliere, M. Papi and A. Laganà, *ACS applied materials & interfaces*, 2013, **5**, 13171-13179.
49. S. W. Provencher, *Computer Physics Communications*, 1982, **27**, 213-227.
50. H. Amenitsch, S. Bernstorff and P. Laggner, *Review of scientific instruments*, 1995, **66**, 1624-1626.
51. G. Ciasca, G. Campi, A. Battisti, G. Rea, M. Rodio, M. Papi, P. Pernot, A. Tenenbaum and A. Bianconi, *Langmuir*, 2012, **28**, 13405-13410.
52. G. Ciasca, M. Papi, M. Chiarpotto, M. Rodio, G. Campi, C. Rossi, P. De Sole and A. Bianconi, *Applied Physics Letters*, 2012, **100**, 073703.
53. F. Bugli, V. Caprettini, M. Cacaci, C. Martini, F. P. Sterbini, R. Torelli, S. Della Longa, M. Papi, V. Palmieri and B. Giardina, *International journal of nanomedicine*, 2014, **9**, 2727.
54. G. Ciasca, L. Businaro, A. De Ninno, A. Cedola, A. Notargiacomo, G. Campi, M. Papi, A. Ranieri, S. Carta and E. Giovine, *Microelectronic Engineering*, 2013, **111**, 304-309.

Graphical abstract

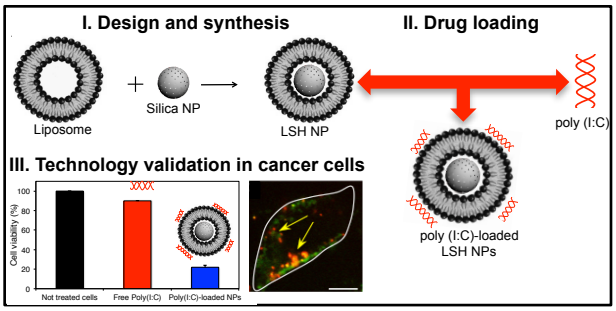

Synthesized core-shell liposome-silica hybrid nanoparticles (LSH NPs), when loaded with the anti-cancer polyinosinic-polycytidylic acid (poly(I:C)), exhibit high anti-tumoral activity in prostate and breast cancer cells.